JOC The Journal of Organic Chemistry

Article

pubs.acs.org/joc

Theoretical Analysis of the Fragmentation of $(CO)_5$: A Symmetry-Allowed Highly Exothermic Reaction that Follows a Stepwise Pathway

Jiajun Liu,[†] Xiaoguang Bao,*[,†] David A. Hrovat,[‡] and Weston Thatcher Borden*[,‡]

[†]College of Chemistry, Chemical Engineering and Materials Science, Soochow University, 199 Ren-Ai Road, Suzhou Industrial Park, Suzhou, Jiangsu 215123, China

[‡]Department of Chemistry and the Center for Advanced Scientific Computing and Modeling, University of North Texas, 1155 Union Circle, #305070, Denton, Texas 76203-5017, United States

Supporting Information

ABSTRACT: B3LYP and CCSD(T) calculations, using an aug-cc-pVTZ basis set, have been carried out on the fragmentation of 1,2,3,4,5-cyclopentanepentone, $(CO)_5$, to five molecules of CO. Although this reaction is calculated to be highly exothermic and is allowed to be concerted by the Woodward–Hoffmann rules, our calculations find that the D_{5h} energy maximum is a multidimensional hilltop on the potential energy surface. This D_{5h} hilltop is 16–20 kcal/mol higher in energy than a C_2 transition structure for the endothermic cleavage of $(CO)_5$ to $(CO)_4$ + CO and 11–15 kcal/mol higher than a C_s transition structure for the loss of two CO molecules. The reasons for the very high energy of the D_{5h} hilltop are discussed, and the geometries of the two lower energy transition structures are rationalized on the basis of mixing of the e_2' HOMO and the a_2'' LUMO of the hilltop.

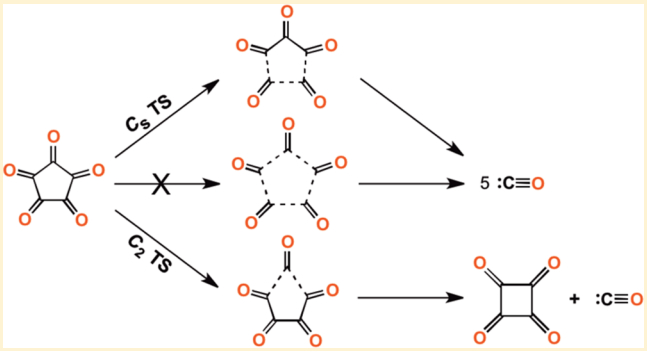

INTRODUCTION

Monocyclic oxocarbons, $(CO)_n$ (n = 3–6), have recently attracted considerable research interest.[1] This interest was initially stimulated by the computational study of the electronic structure of the $(CO)_4$ molecule. Calculations on $(CO)_4$ by Gleiter[2] and Jiao[3] and, subsequently, by us[4] and by Bartlett[5] led to the unexpected conclusion that this apparently normal tetraketone has a triplet ground state.

The reason for this finding is that the two frontier MOs of $(CO)_4$, the b_{2g} σ MO and the a_{2u} π MO in Figure 1, have nearly

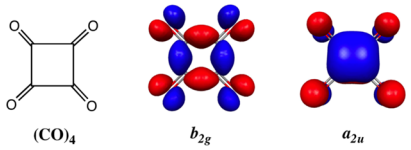

Figure 1. Two frontier MOs of $(CO)_4$, each of which is singly occupied in the triplet ground state of this molecule.

the same energies.[4b,6] These MOs are nondisjoint (i.e., they have atoms in common);[7] therefore, Hund's rule[8] should apply. Consequently, the ground state of $(CO)_4$ was predicted to be a triplet, in which the b_{2g} σ MO and the a_{2u} π MO are each singly occupied.[4b] Recently, Wang and co-workers confirmed this computational conclusion experimentally by using negative-ion photoelectron spectroscopy (NIPES).[9]

Both qualitative MO analysis of and quantitative calculations on the n = 3, 5, and 6 members of the $(CO)_n$ series predicted that, unlike $(CO)_4$, each of these three cyclic oxocarbons has a singlet ground state.[6] NIPES studies of $(CO)_3$,[10] as well as $(CO)_5$ and $(CO)_6$[9b] by Wang once again confirmed these theoretical predictions.

The widths of the peaks in the NIPE spectrum of $(CO)_3$ confirmed a second prediction, namely, that a D_{3h} geometry is not an energy minimum for either the lowest singlet or triplet state of this molecule.[10] The $^3E'$ state undergoes a first-order Jahn–Teller e′ distortion from D_{3h} symmetry before fragmenting to CO plus triplet C_2O_2, and the $^1A_1'$ singlet undergoes a second-order e″ distortion in fragmenting to three molecules of CO. Consequently, a D_{3h} geometry is a hilltop on the potential energy surface for the singlet.

The non-least-motion fragmentation of singlet $(CO)_3$ is interesting because, in a reaction mechanism that preserves D_{3h} symmetry, the MOs of the reactant correlate with the MOs of the product.[6] Consequently, concerted, least-motion fragmentation of $(CO)_3$ to three molecules of CO is a Woodward–Hoffmann allowed reaction.[11] Nevertheless, the D_{3h} fragmenta-

Special Issue: 50 Years and Counting: The Woodward-Hoffmann Rules in the 21st Century

Received: July 7, 2015
Published: September 16, 2015

DOI: 10.1021/acs.joc.5b01546
J. Org. Chem. 2015, 80, 11788–11793

tion pathway is calculated to encounter a barrier, albeit a small one. Consequently, the preferred fragmentation pathways for the singlet involve out-of-plane e″ distortions, which allow the mixing of the filled e′ orbitals of the C−C ring bonds with the low-lying empty a_2'' π MO.[10]

The least-motion fragmentation of singlet $(CO)_5$ is also an orbital-symmetry-allowed reaction in D_{5h} symmetry.[6] We wondered whether if, nevertheless, this fragmentation reaction would, like the fragmentation of $(CO)_3$, be found to prefer a reaction pathway in which symmetry is broken so that C−C bond cleavage is asynchronous.

In this article, we report the results of our computational investigation of this question. We find that a geometry with D_{5h} symmetry is, indeed, a multidimensional hilltop on the potential energy surface for $(CO)_5$ and that the actual transition structures for fragmentation have lower symmetry. The mixing between the e_2' HOMO and the a_2'' LUMO that occurs on e_2'' distortions from D_{5h} symmetry results in C_2 and C_s transition structures both being much lower in energy than the D_{5h} hilltop for synchronous fragmentation.

COMPUTATIONAL METHODOLOGY

Two different types of calculations were carried out in order to investigate the potential energy surface for fragmentation of $(CO)_5$. One set of calculations was based on density functional theory (DFT) and employed the B3LYP functional.[12] The other used CCSD(T).[13] Both sets of calculations were carried out with the aug-cc-pVTZ basis set.[14] Vibrational analyses were performed at all B3LYP stationary points in order to identify each geometry as an energy minimum, transition structure, or hilltop, and the calculated frequencies yielded the zero-point vibrational energy (ZPE) correction for each B3LYP stationary point.

The geometries of the $(CO)_5$ reactant and the products formed from it were also optimized at the CCSD(T)/aug-cc-pVTZ level of theory. Single-point CCSD(T) calculations were performed at the B3LYP geometries for species with one or more imaginary vibrational frequencies. All calculations were carried out with the Gaussian 09 suite of programs.[15]

RESULTS AND DISCUSSION

The results of the B3LYP/aug-cc-pVTZ and CCSD(T)/aug-cc-pVTZ calculations are summarized in Table 1. Complete information about the geometries of all stationary points and the absolute electronic and vibrational energies computed at these geometries is available in the Supporting Information.

Table 1. B3LYP/aug-cc-pVTZ and CCSD(T)/aug-cc-pVTZ Energies (kcal/mol) of the Stationary Points on the Potential Surface for Fragmentation of D_{5h} $(CO)_5$ Relative to the Energy of $(CO)_5$

calculation	D_{5h} MDHT[a]	C_2 TS	C_s TS	$(CO)_4$ + CO	5 CO
B3LYP	55.2	35.5	41.9	7.7[b]	−26.4
CCSD(T)	62.2	46.2[c]	51.0[c]	13.1[c,d]	−35.2

[a]Multidimensional hilltop. The imaginary frequencies and the vibrations to which they correspond are given in the text. [b]Lowest singlet, in which the a_{2u} π MO is doubly occupied. [c]CCSD(T)/aug-cc-pVTZ//B3LYP/aug-cc-pVTZ result. [d]Lowest singlet, in which the b_{2g} σ MO is doubly occupied.

Concerted Fragmentation of $(CO)_5$ in D_{5h} Symmetry. A D_{5h} energy maximum on the potential energy surface for the concerted fragmentation of D_{5h} $(CO)_5$ to five CO molecules was found. At this geometry, the C−C bonds are lengthened to 2.021 Å from 1.555 Å at the B3LYP equilibrium geometry of the reactant, whereas the CO bonds are shortened to 1.149 Å from 1.194 Å in the reactant. The 0.045 Å shortening of the CO bonds is clearly due to partial formation of a second π bond in the molecular plane. The B3LYP/aug-cc-pVTZ bond length in CO is 1.126 Å, which is 0.023 Å shorter than that calculated at the D_{5h} energy maximum.

At the D_{5h} energy maximum, in addition to the expected imaginary frequency (i349.1 cm^{-1}) for the a_1' vibration that connects $(CO)_5$ to five CO molecules, imaginary frequencies of i277.5 and i140.7 cm^{-1} were also found. These latter two imaginary frequencies are, respectively, for a pair of e_2'' and a pair of e_1'' degenerate vibrations. Thus, the D_{5h} energy maximum is not a transition structure on the global potential energy surface for $(CO)_5$. Instead, it is a multidimensional hilltop whose energy can be lowered by geometry distortions along not only an a_1' vibrational coordinate for fragmentation but also along two pairs of degenerate e_1'' and e_2'' vibrational coordinates.

Distortions from D_{5h} Symmetry. The e_1'' and e_2'' vibrations each consist of a degenerate pair of out-of-plane distortions from D_{5h} symmetry. These distortions are shown schematically in Figure 2. The components that maintain a C_2 axis of symmetry are labeled e_{1x}'' and e_{2x}'' in Figure 2. The components that maintain a C_s plane of symmetry are labeled e_{1y}'' and e_{2y}''.

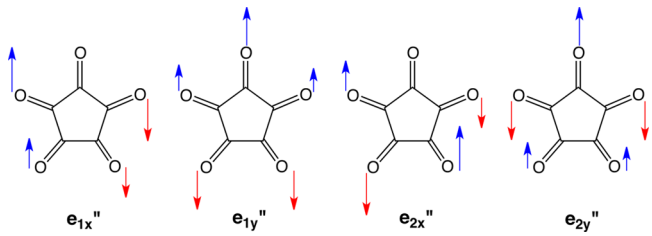

Figure 2. Schematic depiction of e_1'' and e_2'' distortions from D_{5h} symmetry. If the blue arrows represent motions of oxygen atoms upward, above the molecular plane, then the red arrows represent motions of oxygen atoms downward, below the molecular plane.

The imaginary frequency of i277.5 cm^{-1} that is associated with an e_2'' distortion from D_{5h} symmetry is about twice the size of the imaginary frequency of i140.7 cm^{-1} that is associated with an e_1'' distortion. Therefore, it seemed likely that e_2'' distortions would lead to lower energy structures than e_1'' distortions would.

In addition, an e_{2x}'' distortion results in all the C−O bonds being staggered, whereas an e_{2y}'' distortion leaves the C−O bonds at C3 and C4 eclipsed. Therefore, we guessed that the lowest energy transition structure for fragmentation of $(CO)_5$ would be an e_{2x}'' distorted structure, which would have C_2 symmetry and in which all of the C−O bonds would be staggered. Consequently, we began by searching for such a transition structure.

The C_2 Transition Structure for Fragmentation of $(CO)_5$. Our search for an e_{2x}'' distorted transition structure led to the stationary point shown in Figure 3. A vibrational analysis confirmed that it has one and only one imaginary frequency (i313.1 cm^{-1}), which corresponds to extrusion of the unique CO group. Therefore, this C_2 geometry is a transition structure for fragmentation of $(CO)_5$.

Starting at this transition structure and following the transition vector led to cyclic $(CO)_4$ + CO. There was no

DOI: 10.1021/acs.joc.5b01546
J. Org. Chem. 2015, 80, 11788−11793

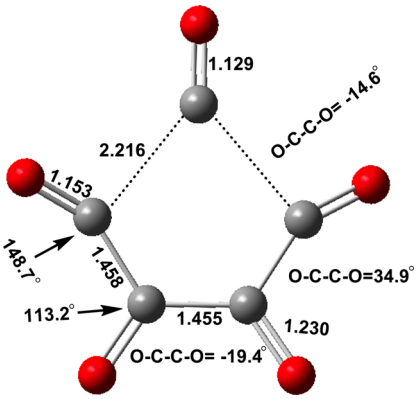

Figure 3. C_2 transition structure for fragmentation of $(CO)_5$. Bond lengths are given in Å, and bond angles and dihedral angles are given in degrees.

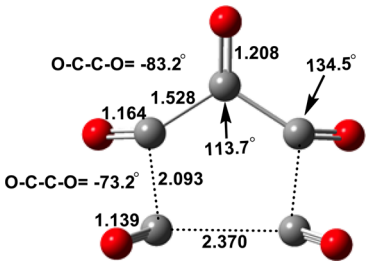

Figure 4. C_s stationary point for fragmentation of $(CO)_5$. Bond lengths are given in Å, and bond angles and dihedral angles are given in degrees.

indication that this transition structure led to further fragmentation of the four-carbon fragment in Figure 3, at least not along a pathway to cyclic $(CO)_4$ that preserves the C_2 axis of symmetry.[16]

As shown in Table 1, the fragmentation of $(CO)_5$ to $(CO)_4$ + CO is calculated at the CCSD(T) level of theory to be endothermic by 13.1 kcal/mol (10.3 kcal/mol including B3LYP corrections for ZPE differences). However, at temperatures high enough to overcome the calculated barrier height of 46.2 kcal/mol, this fragmentation reaction would be thermodynamically favorable because the entropy of $(CO)_4$ + CO is computed to be higher than that of $(CO)_5$ by 39.1 eu.

If cyclic $(CO)_4$ were actually formed in the fragmentation of $(CO)_5$, then it would not survive the reaction conditions. As already noted, cyclic $(CO)_4$ has a triplet ground state,[9] and the triplet is predicted to undergo stepwise fragmentation with a low reaction barrier.[6] However, even if pyrolysis of $(CO)_5$ were to result in the formation of five molecules of CO, the predicted formation of $(CO)_4$ as an intermediate would make the pathway for the fragmentation reaction stepwise, rather than concerted.

The concerted fragmentation of $(CO)_5$ to five molecules of CO is not only a Woodward–Hoffmann allowed reaction[11] but also a reaction that is computed to be 34–48 kcal/mol more enthalpically favorable than fragmentation of $(CO)_5$ to $(CO)_4$ + CO. Nevertheless, the results in Table 1 indicate that the latter pathway is predicted to have a reaction barrier that is lower by 16–20 kcal/mol than that for concerted fragmentation.

The C_s Transition Structure for Fragmentation of $(CO)_5$. Our search for an e_{2y}'' distorted transition structure with a C_s plane of symmetry led to the structure shown in Figure 4. Vibrational analysis confirmed that it has an imaginary frequency of i227.4 cm^{-1} for extrusion of two CO groups and formation of a C_3O_3 fragment. Starting at the C_s structure in Figure 4 and following the vibration with this imaginary frequency led to the subsequent breaking of the two C–C bonds between the three CO groups and eventual formation of five molecules of CO.[17]

This fragmentation pathway from $(CO)_5$ to five molecules of CO does not involve the formation of any intermediates. Therefore, it is energetically concerted. However, breaking of the C–C bonds in $(CO)_5$ via the C_s transition structure in Figure 4 is highly asynchronous. According to Table 1, the barrier for this asynchronous reaction pathway is 11–13 kcal/mol lower in energy than the D_{5h} mountain top for synchronous C–C bond breaking, but the C_s transition structure is 5–6 kcal/mol higher in energy than the C_2 transition structure, which leads to CO plus cyclic $(CO)_4$.

The C_s structure in Figure 4 is actually not a true transition structure because it has a second imaginary frequency of i23.0. This small imaginary frequency corresponds to an antisymmetric vibration that staggers the C–O bonds at C3 and C4. Therefore, the true transition structure has no (i.e., C_1) symmetry. Its structure is given in the Supporting Information.

However, the B3LYP energy of the C_1 transition structure is lower than that of the C_s hilltop in Figure 4 by only 0.1 kcal/mol. Therefore, we prefer to base the following discussion of the transition structures for fragmentation of $(CO)_5$ on the C_s structure in Figure 4 rather than on the C_1 structure described in the Supporting Information.

Why Are the C_2 and C_s Transition Structures Lower in Energy than the D_{5h} Hilltop for Fragmentation? The e_2'' distortions that lead from the D_{5h} hilltop to the C_2 and C_s structures in, respectively, Figures 3 and 4 may be regarded as second-order Jahn–Teller (SOJT) distortions.[18] Each distortion has the correct symmetry to mix one of the degenerate pair of e_2' HOMOs with the a_2'' out-of-plane, CO, π^* LUMO. These MOs are shown in Figure 5.

As shown in Figure 5, the e_2' HOMOs of D_{5h} $(CO)_5$ correlate with the e_2' symmetry combinations of carbon lone-pair MOs on five CO molecules. These lone-pair combinations, which are pictured in Figure 5c, are highly C–C antibonding,

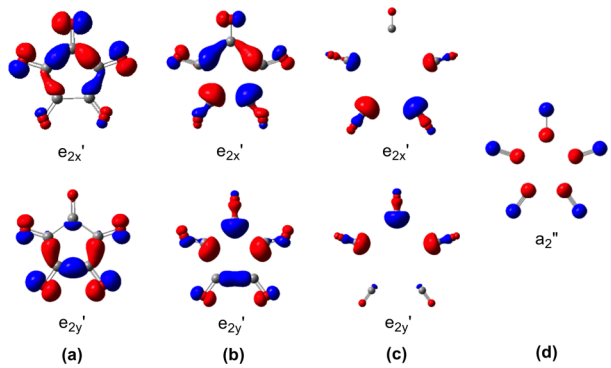

Figure 5. Degenerate e_2' HOMOs of $(CO)_5$ at (a) the equilibrium geometry, (b) the D_{5h} hilltop geometry, and (c) at infinite separation, where the HOMOs are the e_2' combinations of the carbon lone-pair AOs in five CO molecules. C1 is the unique carbon atom in each MO. The a_2'' out-of-plane, CO, π^* LUMO, which remains unchanged in shape at all three geometries, is shown in (d).

DOI: 10.1021/acs.joc.5b01546
J. Org. Chem. 2015, 80, 11788–11793

but, by mixing with the e_2' combinations of in-plane CO π^* MOs, they become the e_2' bonding σ MOs of $(CO)_5$.[6]

Figure 5 shows that the amount of mixing between the carbon lone-pair orbitals and the in-plane CO π^* MOs in the e_2' MOs of D_{5h} $(CO)_5$ depends on the C−C distance. As the C−C distance increases, the mixing between the carbon lone-pair orbitals and the in-plane CO π^* MOs decreases, so the amount of C−C bonding in the e_2' MOs decreases. As the energy of this degenerate pair of HOMOs increases, the energy gap between them and the a_2'' LUMO decreases.

The smaller the HOMO−LUMO energy gap, the more favorable the SOJT mixing between the e_2' σ MOs and the a_2'' π MO becomes. That is why the e_2'' vibrations, which cause the SOJT mixing of these MOs, have a positive force constant and a real frequency of 34.6 cm^{-1} at the D_{5h} equilibrium geometry, but they have a negative force constant and an imaginary frequency of i277.5 cm^{-1} at the D_{5h} hilltop.

How does the SOJT mixing of the degenerate e_2' HOMOs with the a_2'' LUMO lower the energy of $(CO)_5$ at the D_{5h} hilltop? As shown in Figure 5b, at this geometry there are serious antibonding interactions in e_2' between the lone-pair AOs on the carbons. These antibonding interactions are mitigated by the mixing of the e_2' HOMOs with the a_2'' LUMO upon an e_2'' molecular distortion.

More specifically, Figure 5b shows that in the e_{2x}' MO at the D_{5h} hilltop there are strong, nearest-neighbor antibonding interactions between the AOs on C2, C3, C4, and C5. These interactions can be mitigated by an e_{2x}'' distortion, which moves the oxygens attached to adjacent carbons in opposite directions above and below the molecular plane. This distortion mixes the e_{2x}' MO with the a_2'' MO and thus reorients the AOs on nearest-neighbor atoms above and below the molecular plane.

This can be seen in Figure 6, which shows the HOMO of $(CO)_5$ at the C_2 transition structure. The large red lobes on C2 and C4 point above the plane of the four carbons, and the large blue lobes at C3 and C5 point below this plane.

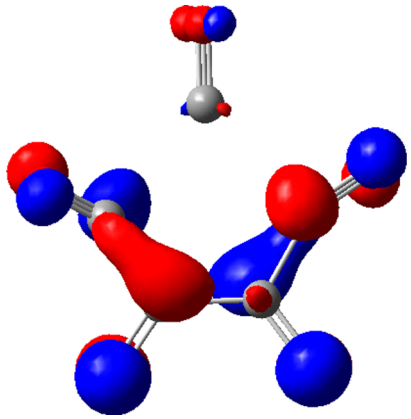

Figure 6. HOMO of the C_2 transition structure for the fragmentation of $(CO)_5$ to $(CO)_4$ + CO. This MO results from SOJT mixing of the e_{2x}' HOMO with the a_2'' LUMO of D_{5h} $(CO)_5$ upon an e_{2x}'' molecular distortion.

An e_{2x}'' molecular distortion does not mix the e_{2y}' HOMO in Figure 5 with the a_2'' LUMO. Consequently, the strongly antibonding interactions of the orbitals on C1 with the orbitals on C2 and C5 in e_{2y}' persist after an e_{2x}'' molecular distortion. In order to alleviate these interactions, the C1−C2 and C1−C5 bonds lengthen, which is why the geometry of the C_2 transition structure has long C−C bond distances to C1.

Although an e_{2x}'' molecular distortion does not mix the e_{2y}' HOMO with the a_2'' LUMO, an e_{2y}'' molecular distortion does result in this mixing. This mixing mitigates the strongly antibonding interactions of the orbital on C1 with the orbitals on C2 and C5 in the e_{2y}' MO and leads to the C_s stationary point in Figure 4. The HOMO at this geometry, which arises from the mixing of the e_{2y}' HOMO with the a_2'' LUMO, is shown in Figure 7. The large blue lobe at C1 points below the C2−C1−C5 plane, and the large red lobes at C2 and C5 point above this plane.

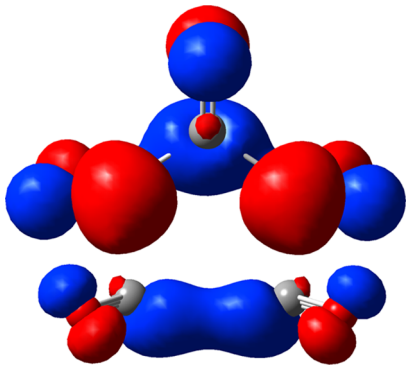

Figure 7. HOMO of the C_s transition structure for the fragmentation of $(CO)_5$ initially to C_3O_3 + 2 CO. This MO results from SOJT mixing of the e_{2y}' HOMO with the a_2'' LUMO of D_{5h} $(CO)_5$ upon an e_{2y}'' molecular distortion.

An e_{2y}'' molecular distortion does not mix the e_{2x}' HOMO in Figure 5 with the a_2'' LUMO. Consequently, the strongly antibonding interactions in e_{2x}' of the orbitals on C3 and C4 with each other and with the orbitals on C2 and C5 persist after an e_{2y}'' molecular distortion. In order to alleviate these interactions, the bonds to C3 and C4 all lengthen, which is why the geometry of the C_s transition structure has long bond distances to these two carbons.

Transition Structures Derived from e_1'' Distortions of the D_{5h} Hilltop Geometry. As already noted, at the D_{5h} hilltop geometry not only e_2'' but also e_1'' vibrations have imaginary frequencies. The degenerate pair of e_1'' distortions has imaginary frequencies because they allow SOJT mixing between the high-lying e_1' MOs and the a_2'' LUMO. This type of out-of-plane distortion mitigates the antibonding interactions between the e_1' combinations of carbon lone-pair AOs at the D_{5h} hilltop geometry.

The degenerate pair of e_1' MOs at the D_{5h} hilltop geometry is shown in Figure 8. Unlike the e_2' MOs, which have two nodal

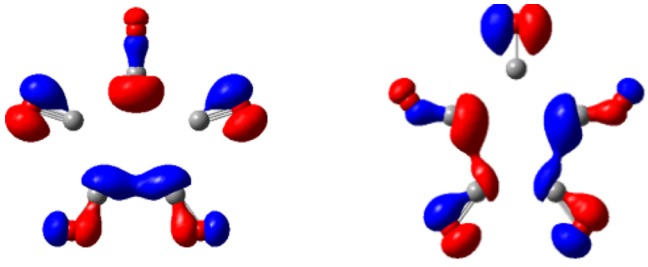

Figure 8. Degenerate e_1' HOMOs of $(CO)_5$ at the D_{5h} hilltop geometry of $(CO)_5$.

DOI: 10.1021/acs.joc.5b01546
J. Org. Chem. 2015, 80, 11788−11793

planes between the carbon lone-pair AOs, the e_1' MOs have just one such plane. This is the reason that the e_1' MOs are lower in energy than the e_2' HOMOs of $(CO)_5$ at the D_{5h} hilltop geometry.

The lower energy of the e_1' MOs than of the e_2' MOs means that the mixing of the a_2'' LUMO with the e_1' MOs upon an e_1'' distortion from D_{5h} symmetry provides less stabilization than the mixing of a_2'' with the e_2' MOs upon an e_2'' distortion from D_{5h} symmetry. This is the reason why at the D_{5h} hilltop geometry an e_1'' vibration has an imaginary frequency that is only about half the size of an e_2'' vibration.

Although we searched for C_2 and C_s transition structures that would represent e_1'' distortions from D_{5h} symmetry, we were unable to find them. Our searches always led back to the C_2 transition structure shown in Figure 3 or to the C_s transition structure shown in Figure 4, each of which represents an e_2'' distortion from D_{5h} symmetry. The much smaller imaginary frequency for an e_1'' distortion than that for an e_2'' distortion from D_{5h} symmetry indicates that, if e_1'' distorted transition structures do exist, then they are almost certainly higher in energy than the e_2'' distorted transition structures that are shown in Figures 3 and 4.

CONCLUSIONS

Despite being allowed by orbital symmetry and being very favorable energetically, fragmentation of $(CO)_5$ to five molecules of CO is calculated not to occur in a synchronous fashion. The D_{5h} energy maximum is not a transition structure but a multidimensional hilltop on the potential energy surface for fragmentation of $(CO)_5$. The hilltop has an imaginary frequency for e_2'' vibrational modes and a much smaller imaginary frequency for e_1'' vibrational modes.

We have located the C_2 and C_s transition structures that come from, respectively, e_{2x}'' and e_{2y}'' distortions of $(CO)_5$ from D_{5h} symmetry. Passage over the lower energy C_2 transition state in Figure 3 results in cleavage of one CO group from $(CO)_5$ and is calculated to lead to the formation of cyclic $(CO)_4$, instead of to four additional molecules of CO.[16] Passage over the higher energy C_s transition state in Figure 4 leads to cleavage of $(CO)_5$ to two molecules of CO plus a C_3O_3 fragment, which subsequently dissociates, without a barrier, to three more molecules of CO.

Unlike the C_2 reaction pathway, the C_s pathway does lead to fragmentation of $(CO)_5$ to five molecules of CO, without formation of any intermediates. Therefore, it is energetically concerted. However, the reaction occurs in two discrete stages—fragmentation of $(CO)_5$ to 2 CO + C_3O_3, followed by barrierless fragmentation of acyclic C_3O_3 to three more molecules of CO. Consequently, the C_s transition structure leads to a fragmentation reaction that is highly asynchronous.

The explanation of why the C_2 and C_s transition structures for stepwise C−C bond breaking provide much lower energy alternatives to a D_{5h} structure for simultaneously cleaving all five bonds in $(CO)_5$ can be understood by inspection of the e_2' HOMO of D_{5h} $(CO)_5$ in Figure 5. The figure shows that, as the C−C bond distances in D_{5h} $(CO)_5$ increase, the contributions of the in-plane C−O π^* MOs to the C−C bonding in $(CO)_5$ decrease. This decrease occurs for two different but closely related reasons.

First, the C−C bonding interactions between the in-plane π^* MOs decrease with increasing C−C distance, thus increasing the energy difference between these empty MOs and the filled e_2' lone-pair orbitals on the carbons. Second, the bonding interactions between the empty in-plane π^* MOs and the filled e_2' lone-pair orbitals on the carbons also decrease. Consequently, as the C−C distances in $(CO)_5$ increase, the bonding interactions between the in-plane C−O π^* MOs and the filled e_2' lone-pair orbitals on the carbons are increasingly dominated by the antibonding interactions of the carbon lone-pair AOs with each other.

These antibonding interactions between the lone pair AOs on the carbons can be ameliorated by e_2'' second-order Jahn−Teller (SOJT) geometry distortions.[18] These distortions allow the filled e_2' HOMO to mix with the a_2'' LUMO, and this mixing reorients the carbon lone-pair AOs in space and reduces the antibonding interactions between them.

The antibonding interactions between the carbon lone pair AOs at the geometry of the D_{5h} hilltop result in its energy being calculated to be 55−62 kcal/mol above that of the $(CO)_5$ reactant and 82−97 kcal/mol above that of five CO molecules. The e_{2x}'' SOJT distortion of the geometry of the D_{5h} hilltop results in the preferred C_2 transition structure being calculated to be 16−20 kcal/mol lower in energy than the hilltop geometry. Extrusion of a single CO molecule from $(CO)_5$ is predicted to be preferred to concerted, synchronous fragmentation of $(CO)_5$ by this amount of energy.

The Woodward−Hoffmann rules for pericyclic reactions[11] would lead one to expect that a highly exothermic fragmentation reaction, which is allowed to be concerted by orbital symmetry, would be greatly favored over a stepwise, endothermic cleavage reaction. The results of our calculations show that this is certainly not the case for $(CO)_5 \rightarrow 5$ CO, where a concerted, exothermic reaction pathway is calculated to be 16−20 kcal/mol higher in energy than a stepwise, endothermic reaction pathway.

A previous example of a reaction that is exothermic and symmetry-allowed being calculated to have a high reaction barrier is the trimerization of acetylene to benzene.[19] In that case, the D_{3h} transition structure is destabilized by the requirement that the acetylenes must undergo significant amounts of *cis* bending before being stabilized by interactions between the high-lying, filled, in-plane π MOs and the low-lying, empty, in-plane π^* MOs.

The fragmentation of $(CO)_5$ is different in that the five CO molecules do not need to undergo geometry distortions in order for the filled carbon lone-pair orbitals to interact with the empty, in-plane C−O π^* MOs. However, the CO molecules must be within about 2.02 Å of each other (the C−C bond lengths at the D_{5h} hilltop) before the bonding created by these lone-pair−π^* interactions begins to overcome the antibonding created by the filled, lone-pair AOs interacting with each other. At the geometry of the D_{5h} hilltop, the carbons are too distant for the lone-pair−π^* interactions to dominate the lone pair repulsions, but they are too close for the lone-pair repulsions not to significantly destabilize this geometry for the concerted fragmentation of $(CO)_5$ to five molecules of CO.

These repulsions between the filled, lone-pair AOs are the reason why the D_{5h} geometry for concerted fragmentation is calculated to be a hilltop, 55−62 kcal/mol above $(CO)_5$, and why the C_2 and C_s geometries, in which these repulsions are mitigated, are the transition structures, leading to fragmentation of $(CO)_5$ in a stepwise fashion.

DOI: 10.1021/acs.joc.5b01546
J. Org. Chem. 2015, 80, 11788−11793

■ ASSOCIATED CONTENT

Supporting Information

The Supporting Information is available free of charge on the ACS Publications website at DOI: 10.1021/acs.joc.5b01546.

Geometries of all stationary points and absolute electronic and vibrational energies computed at these geometries (PDF).

■ AUTHOR INFORMATION

Corresponding Authors

*(X.B.) E-mail: xgbao@suda.edu.cn.
*(W.T.B.) E-mail: borden@unt.edu.

Notes

The authors declare no competing financial interest.

■ ACKNOWLEDGMENTS

The research at the Soochow University was supported by grants to X.B. from the Natural Science Foundation of China (NSFC 21302133) and the Priority Academic Program Development of Jiangsu Higher Education Institutions (PAPD). The research at the University of North Texas was supported by grant B0027 from the Robert A. Welch Foundation to W.T.B.

■ REFERENCES

(1) For a review, see Borden, W. T. *Isr. J. Chem.* **2015**, DOI: 10.1002/ijch.201400170.

(2) Gleiter, R.; Hyla-Kryspin, I.; Pfeifer, K.-H. *J. Org. Chem.* **1995**, *60*, 5878.

(3) Jiao, H.; Frapper, G.; Halet, J.-F.; Saillard, J.-Y. *J. Phys. Chem. A* **2001**, *105*, 5945.

(4) (a) Zhou, X.; Hrovat, D. A.; Gleiter, R.; Borden, W. T. *Mol. Phys.* **2009**, *107*, 863. (b) Zhou, X.; Hrovat, D. A.; Borden, W. T. *J. Phys. Chem. A* **2010**, *114*, 1304.

(5) Perera, A.; Molt, R. W., Jr.; Lotrich, V. F.; Bartlett, R. J. *Theor. Chem. Acc.* **2014**, *133*, 1514.

(6) Bao, X.; Zhou, X.; Lovitt, C. F.; Venkatraman, A.; Hrovat, D. A.; Gleiter, R.; Hoffmann, R.; Borden, W. T. *J. Am. Chem. Soc.* **2012**, *134*, 10259.

(7) (a) Borden, W. T.; Davidson, E. R. *J. Am. Chem. Soc.* **1977**, *99*, 4587. (b) Borden, W. T. In *Diradicals*; Borden, W. T., Ed.; Wiley-Interscience: New York, 1982; pp 1−72.

(8) Review: Kutzelnigg, W. *Angew. Chem., Int. Ed. Engl.* **1996**, *35*, 572.

(9) (a) Guo, J.-C.; Hou, G.-L.; Li, S. D.; Wang, X.-B. *J. Phys. Chem. Lett.* **2012**, *3*, 304. (b) Bao, X.; Hrovat, D. A.; Borden, W. T.; Wang, X.-B. *J. Am. Chem. Soc.* **2013**, *135*, 4291.

(10) Chen, B.; Hrovat, D. A.; West, R.; Deng, S. H. M.; Wang, X.-B.; Borden, W. T. *J. Am. Chem. Soc.* **2014**, *136*, 12345.

(11) Review: Woodward, R. B.; Hoffmann, R. *Angew. Chem., Int. Ed. Engl.* **1969**, *8*, 781.

(12) (a) Becke, A. D. *J. Chem. Phys.* **1993**, *98*, 5648. (b) Lee, C.; Yang, W.; Parr, R. G. *Phys. Rev. B: Condens. Matter Mater. Phys.* **1988**, *37*, 785.

(13) (a) Purvis, G. D.; Bartlett, R. J. *J. Chem. Phys.* **1982**, *76*, 1910. (b) Raghavachari, K.; Trucks, G. W.; Pople, J. A.; Head-Gordon, M. H. *Chem. Phys. Lett.* **1989**, *157*, 479.

(14) (a) Dunning, T. H., Jr. *J. Chem. Phys.* **1989**, *90*, 1007. (b) Kendall, R. A.; Dunning, T. H., Jr.; Harrison, R. J. *J. Chem. Phys.* **1992**, *96*, 6796.

(15) Frisch, M. J.; Trucks, G. W.; Schlegel, H. B.; Scuseria, G. E.; Robb, M. A.; Cheeseman, J. R.; Scalmani, G.; Barone, V.; Mennucci, B.; Petersson, G. A.; Nakatsuji, H.; Caricato, M.; Li, X.; Hratchian, H. P.; Izmaylov, A. F.; Bloino, J.; Zheng, G.; Sonnenberg, J. L.; Hada, M.; Ehara, M.; Toyota, K.; Fukuda, R.; Hasegawa, J.; Ishida, M.; Nakajima, T.; Honda, Y.; Kitao, O.; Nakai, H.; Vreven, T.; Montgomery, J. A., Jr.; Peralta, J. E.; Ogliaro, F.; Bearpark, M.; Heyd, J. J.; Brothers, E.; Kudin, K. N.; Staroverov, V. N.; Kobayashi, R.; Normand, J.; Raghavachari, K.; Rendell, A.; Burant, J. C.; Iyengar, S. S.; Tomasi, J.; Cossi, M.; Rega, N.; Millam, J. M.; Klene, M.; Knox, J. E.; Cross, J. B.; Bakken, V.; Adamo, C.; Jaramillo, J.; Gomperts, R.; Stratmann, R. E.; Yazyev, O.; Austin, A. J.; Cammi, R.; Pomelli, C.; Ochterski, J. W.; Martin, R. L.; Morokuma, K.; Zakrzewski, V. G.; Voth, G. A.; Salvador, P.; Dannenberg, J. J.; Dapprich, S.; Daniels, A. D.; Farkas, O.; Foresman, J. B.; Ortiz, J. V.; Cioslowski, J.; Fox, D. J. *Gaussian 09*, revision D.01; Gaussian, Inc.: Wallingford, CT, 2009.

(16) At the B3LYP level of theory, the lowest singlet state of cyclic $(CO)_4$ has 10 π electrons, with the a_{2u} π^* MO doubly occupied and the b_{2g} σ MO empty.[4a] Although the C_4O_4 fragment in Figure 3 lacks the plane of symmetry that would differentiate between a σ and a π MO, inspection of the HOMO of the C_4O_4 fragment (Figure 6) indicates that this doubly occupied MO correlates with the a_{2u} π^* MO of cyclic $(CO)_4$. The nature of the HOMO of the C_4O_4 fragment explains not only why the ring closure reaction proceeds without a barrier but also why the C_4O_4 fragment is calculated to close rather than to dissociate to four molecules of CO.

(17) Previous calculations and experiments have found that ring opening and fragmentation of cyclic $(CO)_3$ is energetically favorable and barrierless.[10] Therefore, ring closure of the C_3O_3 fragment in Figure 4 would not be expected to occur since acyclic C_3O_3 is lower in energy than cyclic $(CO)_3$.

(18) See, *inter alia*, (a) Öpik, U.; Pryce, M. H. L. *Proc. R. Soc. London, Ser. A* **1957**, *238*, 425. (b) Bader, R. F. W. *Can. J. Chem.* **1962**, *40*, 1164. (c) Pearson, R. G. *J. Am. Chem. Soc.* **1969**, *91*, 4947. (d) Pearson, R. G. *J. Mol. Struct.: THEOCHEM* **1983**, *103*, 25. For a recent review, see: (e) Bersuker, I. B. *Chem. Rev.* **2013**, *113*, 1351.

(19) (a) Houk, K. N.; Gandour, R. W.; Strozier, R. W.; Rondan, N. G.; Paquette, L. A. *J. Am. Chem. Soc.* **1979**, *101*, 6797. (b) Bach, R. D.; Wolber, G. J.; Schlegel, H. B. *J. Am. Chem. Soc.* **1985**, *107*, 2837. (c) Ioffe, A.; Shaik, S. *J. Chem. Soc., Perkin Trans. 2* **1992**, *2*, 2101. (d) Wagenseller, P. E.; Birney, D. M.; Roy, D. *J. Org. Chem.* **1995**, *60*, 2853. (e) Jiao, H.; Schleyer, P. v. R. *J. Phys. Org. Chem.* **1998**, *11*, 655. (f) Morao, I.; Cossio, F. *J. Org. Chem.* **1999**, *64*, 1868. (g) Sawicka, D.; Wilsey, S.; Houk, K. N. *J. Am. Chem. Soc.* **1999**, *121*, 864. (h) Sawicka, D.; Li, Y.; Houk, K. N. *J. Chem. Soc., Perkin Trans. 2* **1999**, *9*, 2349. (i) Cioslowski, J.; Liu, G.; Moncrieff, D. *Chem. Phys. Lett.* **2000**, *316*, 536. (j) Havenith, R.; Fowler, P.; Jenneskens, L.; Steiner, E. *J. Phys. Chem. A* **2003**, *107*, 1867. (k) Santos, J. C.; Polo, V.; Andres, J. *Chem. Phys. Lett.* **2005**, *406*, 393. (l) Eichberg, M. J.; Houk, K. N.; Lehmann, J.; Leonard, P. W.; Marker, A.; Norton, J. E.; Sawicka, D.; Vollhardt, K. P. C.; Whitener, G. D.; Wolff, S. *Angew. Chem., Int. Ed.* **2007**, *46*, 6894. (m) Donoso-Tauda, O.; Aizman, A.; Escobar, C. A.; Santos, J. C. *Chem. Phys. Lett.* **2009**, *469*, 219. (n) Sakai, S.; Udagawa, T.; Kato, S.; Nakada, K. *J. Phys. Org. Chem.* **2013**, *26*, 517.

DOI: 10.1021/acs.joc.5b01546
J. Org. Chem. 2015, 80, 11788−11793